

This document is confidential and is proprietary to the American Chemical Society and its authors. Do not copy or disclose without written permission. If you have received this item in error, notify the sender and delete all copies.

***In Vacuo* Porphyrin Metalation on Ag(111) via Chemical Vapor Deposition of Ru₃(CO)₁₂: Mechanistic Insights**

Journal:	<i>The Journal of Physical Chemistry</i>
Manuscript ID	jp-2016-01457v.R1
Manuscript Type:	Article
Date Submitted by the Author:	n/a
Complete List of Authors:	<p>Papageorgiou, Anthoula; Technische Universität München, Physik Department E20 Diller, Katharina; École polytechnique fédérale de Lausanne, Institute of Condensed Matter Physics Fischer, Sybille; Technical University of Munich, Physics Department Allegretti, Francesco; Technical University of Munich, Physics Department E20 Klappenberger, Florian; TU-München, Physics Department Oh, Seung Cheol; Technische Universität München, Sağlam, Özge; Technische Universität München, Physik Department E20 Reichert, Joachim; TUM, Physik Department E20 Wiengarten, Alissa; Technical University Munich, Seufert, Knud; Technische Universität München, Physik Department E20 Auwärter, Willi; Technische Universität München, Physik Department E20 Barth, Johannes; TU München, Physics</p>

SCHOLARONE™
Manuscripts

1
2
3
4
5
6
7
8
9
10
11
12
13
14
15
16
17
18
19
20
21
22
23
24
25
26
27
28
29
30
31
32
33
34
35
36
37
38
39
40
41
42
43
44
45
46
47
48
49
50
51
52
53
54
55
56
57
58
59
60

In Vacuo Porphyrin Metalation on Ag(111) *via* Chemical Vapor Deposition of Ru₃(CO)₁₂: Mechanistic Insights

Anthoula C. Papageorgiou, Katharina Diller,† Sybille Fischer, Francesco Allegretti,
Florian Klappenberger, Seung Cheol Oh, Özge Sağlam,‡ Joachim Reichert,* Alissa
Wiengarten, Knud Seufert, Willi Auwärter, and Johannes V. Barth*

AUTHOR ADDRESS. Physik-Department E20, Technische Universität München, D-85748
Garching, Germany

AUTHOR INFORMATION

Corresponding Author

* Email: a.c.papageorgiou@tum.de (A.C.P.), joachim.reichert@tum.de (J.R.). Telephone
numbers: +49-89-289-12618 (A.C.P.), +49-89-289-12618-12443 (J.R.)

Present Addresses

† Institute of Condensed Matter Physics (ICMP), École Polytechnique Fédérale de Lausanne
(EPFL), Station 3, CH-1015 Lausanne, Switzerland. ‡ Faculty of Engineering and Computer
Sciences, Izmir University of Economics, Sakarya Cad.156, Balcova, Izmir, Turkey.

1
2
3 **ABSTRACT.** Porphyrin molecules offer a very stable molecular environment for the
4 incorporation of numerous metal ions inside their cavity, which enables a plethora of
5 applications. The fabrication and characterization of surface confined metal-organic
6 architectures by employing porphyrins are of particular interest. Here we report on a
7 comprehensive study of chemical vapor deposition (CVD) of triruthenium dodecacarbonyl as
8 metal precursor for the on-surface metalation of different porphyrin species with Ru under
9 ultra-high vacuum conditions. By employing synchrotron radiation X-ray photoelectron
10 spectroscopy (XPS), near-edge X-ray absorption fine structure (NEXAFS) and scanning
11 tunneling spectroscopy (STM), we investigated the metalation process and particularly the
12 role of the support: the close packed Ag(111) surface. It was found that the surface is active
13 in the metalation process under the employed conditions: it decomposes the metal precursor
14 and delivers metal centers to the porphyrin macrocycles. The generality of the metalation
15 process is illustrated for tetraphenylporphyrin, its high temperature derivatives and porphine.
16
17
18
19
20
21
22
23
24
25
26
27
28
29
30
31
32
33
34
35
36
37
38
39
40
41
42
43
44
45
46
47
48
49
50
51
52
53
54
55
56
57
58
59
60

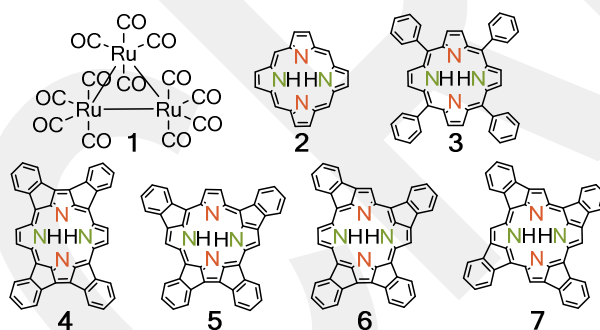
INTRODUCTION

1
2
3
4
5 Porphyrin molecules are natural products, with their tetrapyrrole macrocycles providing a
6 well-defined coordination environment for a vast array of reducible metal centers.
7
8 Biologically important tetrapyrrole macrocycles serve as prosthetic groups in hemoglobin
9 (iron porphyrin) and photosystems (magnesium chlorin), which perform the transport of
10 respiratory gases and energy conversion functions, respectively. These functions depend
11 strongly on the type of hosted metal center.
12
13
14
15
16
17

18 Porphyrins at interfaces, and in particular their electronic properties and their metalation,
19 have been extensively studied.¹⁻⁴ On surfaces, the porphyrin metalation is most frequently
20 achieved by physical vapor deposition of the desired metal atoms⁵⁻⁷ or by capturing surface
21 (ad)atoms, the so-called “self-metalation”.⁸⁻⁹ In an effort to metalate porphyrins on surfaces
22 using metals with high sublimation temperature (e.g. Ru and Os) without being restricted by
23 the supporting surface, we devised a different approach by employing metal-organic
24 chemical vapor deposition (CVD) to metalate porphyrins on Ag(111) with trimetal
25 dodecacarbonyls,¹⁰⁻¹¹ which are stable in air and thermally decompose on surfaces forming
26 metal clusters.¹²⁻¹³ More recently, CVD of metal carbonyl precursors was demonstrated to
27 further provide a route for the on-surface one-dimensional supramolecular assembly of
28 carbonitrile ditopic linker molecules.¹⁴
29
30
31
32
33
34
35
36
37
38
39
40
41
42

43 Our earlier multitechnique study showed a self-terminating protocol, whereby following two
44 cycles of exposure of a layer of the cyclodehydrogenated *meso*-tetraphenylporphyrin (**4**, **5**, **6**,
45 **7**, Figure 1) to the organometallic precursor molecule $\text{Ru}_3(\text{CO})_{12}$ (**1**) and subsequent
46 annealing to 550 K, all free-base species transformed to ruthenium porphyrins without
47 leaving by-products (such as CO and excess Ru) on the surface.¹⁰ Here we elucidate the
48 reaction pathway of this metalation method. In particular, we investigate the role of the silver
49 surface in the process. To this end, the thermal chemistry of pristine $\text{Ru}_3(\text{CO})_{12}$ molecules
50
51
52
53
54
55
56
57
58
59
60

1
2
3 adsorbed on Ag(111) and the metalation as a function of the free Ag(111) surface are
4 investigated. The metalation process was monitored with XPS, while NEXAFS
5 measurements were primarily used to distinguish between 2H-TPP and its planar derivatives.
6
7
8 Furthermore, the metalation of pristine 2H-TPP (**3**, Figure 1) *via* Ru₃(CO)₁₂ is explored with
9 XPS, NEXAFS and STM. Additional information is provided by the XPS and NEXAFS
10 characterization of a monolayer and multilayers of purchased Ru(CO)-TPP. Finally, we look
11 into the 2H-P (**2**, Figure 1) metalation with Ru₃(CO)₁₂ on Ag(111) and assess the relevant
12 results in comparison to the respective Ru metalation of 2H-TPP and its planar derivatives.
13
14 Thus the generality of the introduced CVD approach and the pertaining mechanism is
15 demonstrated.
16
17
18
19
20
21
22
23
24
25
26
27



40 **Figure 1.** Molecular structures of the Ru₃(CO)₁₂ metal precursor **1**, porphine (2H-P) **2**, *meso*-
41 tetraphenylporphyrin (2H-TPP) **3**, and the planar 2H-TPP derivatives **4**, **5**, **6**, **7**. Green and
42 orange indicate the aminic and iminic N sites of the porphyrin macrocycle, respectively.
43
44
45
46

47 METHODS

48
49 Clean Ag(111) single-crystal (Surface Preparation Laboratory) surfaces were prepared by
50 repeated cycles of Ar⁺ sputtering and annealing, as confirmed by XPS (synchrotron
51 measurements at BESSY II) or STM (at TUM). *meso*-Tetraphenylporphyrin (2H-TPP, **3**)
52 (Sigma-Aldrich, ≥99%) was dosed by organic molecular beam epitaxy (*in vacuo* sublimation
53
54
55
56
57
58
59
60

1
2
3 temperatures of 600-620 K). The Ag(111) surface was kept at room temperature (RT) to
4
5 obtain pristine 2H-TPP layers or at 550 K to obtain ~ 1 ML (where 1 ML corresponds to the
6
7 minimum molecular coverage required to completely cover the silver surface) of the planar
8
9 2H-TPP derivatives (**4**, **5**, **6**, **7**). As in our earlier work,¹⁰ triruthenium dodecacarbonyl, **1**,
10
11 (Aldrich, 99%) was dosed by exposure of the porphyrin film on Ag(111) to the vapor of the
12
13 molecule at RT in a vacuum of $\sim 5 \times 10^{-8}$ mbar (BESSY II) or $\sim 6 \times 10^{-10}$ mbar (TUM). The
14
15 temperature of the sample was monitored by type K thermocouple in direct contact with the
16
17 silver single crystal. The duration of the annealing treatments reported in the results and
18
19 discussion section below was ~ 10 min at the reported temperature.
20
21

22
23 STM measurements were carried out in two separate custom-made UHV systems with a
24
25 CreaTec Fischer LT-STM operated at 7 K and an Aarhus 150 VT-STM operated at 95-300 K.
26
27 The base pressure during the experiments was $< 2 \times 10^{-10}$ mbar in the LT-STM and $< 5 \times 10^{-10}$
28
29 mbar in the VT-STM. All STM images were recorded in constant-current mode using
30
31 electrochemically etched tungsten tips. The tunneling bias (V_s) is applied to the sample. The
32
33 WsXM program (www.nanotec.es) was used to process the STM images.
34
35

36
37 Synchrotron XPS and NEXAFS measurements were carried out at the HE-SGM
38
39 monochromator dipole magnet beamline at the BESSY II synchrotron radiation source in
40
41 Berlin, which provides light with a linear polarization of 90%. Photoelectron spectra were
42
43 collected using a Scienta R3000 electron energy analyzer. The angle between the analyzer
44
45 entrance lens and the incoming photon beam was 45° in the horizontal plane. All spectra
46
47 were recorded in normal emission with the sample held approximately at RT. The excitation
48
49 energies used for the acquisition of the regions of N 1s, O 1s, and C 1s & Ru 3d spectra were
50
51 550, 680, and 435 eV, respectively. The binding energy scale of the XP spectra was
52
53 calibrated against the Ag 3d_{5/2} line at 368.3 eV. A polynomial background was subtracted
54
55 from the raw N 1s spectra¹⁵ to compensate the background of Ag 3d shakeup satellites^{13, 16} or
56
57
58
59
60

1
2
3 plasmons,¹⁷ which is exacerbated by the low signal of N 1s at submonolayer coverages. The
4
5 raw data with corrected binding energy scale of all the N 1s regions presented in this
6
7 manuscript can be found in the Supporting Information (Figure S1). The reference for the
8
9 monolayer calibration in the synchrotron measurements is given by the C 1s and N 1s signals
10
11 of a saturated layer of planar 2H-TPP derivatives. Angle-dependent NEXAFS spectra were
12
13 acquired in partial electron yield mode varying the orientation of the light polarization
14
15 relative to the surface normal (further details are given in the Supporting Information).
16
17

18 RESULTS AND DISCUSSION

19
20 **Ru₃(CO)₁₂ on Ag(111).** We will first address the adsorption and thermal chemistry of the
21
22 precursor Ru₃(CO)₁₂ on the pristine Ag(111) without the presence of porphyrins. Directly
23
24 after deposition at RT (Figure 2a) three main features at 280.7 eV, 284.8 and 286.5 eV can be
25
26 identified in the C 1s and Ru 3d core-level region, which are assigned to the Ru 3d doublet
27
28 and the CO C 1s singlet contribution, respectively.¹⁸⁻¹⁹ Both the Ru 3d_{5/2} and 3d_{3/2} core levels
29
30 are split into two components. We attribute this splitting to the inequivalent interaction of the
31
32 Ru atoms of the precursor molecule (**1**) and the Ag(111) surface. Consistently, a single broad
33
34 peak originating from CO is observed in the O 1s region. Stepwise annealing of the sample to
35
36 ~ 500 K (Figure 2b-d) leads to a gradual decrease of the C 1s signal and a shift of the whole
37
38 spectrum to lower binding energies. After annealing to 540 K (Figure 2e) no CO can be
39
40 detected and the Ru peaks appear much sharper. Concomitantly, the total amount of
41
42 ruthenium decreases by a factor of two during the whole annealing process. Together with the
43
44 Ru 3d_{5/2} binding energy of 280.0 eV, which is indicative of Ru⁰ (see ref. ²⁰) these results
45
46 show that annealing leads to desorption of the labile CO ligands and the formation of metallic
47
48 ruthenium. This is consistent with annealing series of Ru₃(CO)₁₂/Co(0001)¹⁸ and
49
50 Ru₃(CO)₁₂/Au(111),¹⁹ which show desorption of CO and a shift to lower binding energies
51
52 upon annealing. In both cases metallic Ru is found after the heat treatment. Deviations from
53
54
55
56
57
58
59
60

the reported binding energies of the as-deposited $\text{Ru}_3(\text{CO})_{12}$ and in the onset of CO desorption might be the results of the modified interaction with the surface. In short, we observe that at the temperature applied in our earlier report on the metalation protocol (550 K),¹⁰ the Ru precursor **1** fully decomposes to metallic Ru on the Ag(111) surface.

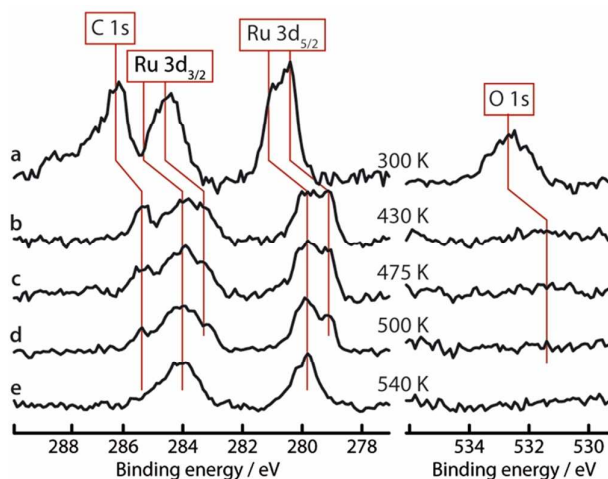


Figure 2. XP spectra of an annealing series of $\text{Ru}_3(\text{CO})_{12}$ on Ag(111). Directly after deposition three main features are discriminable: The Ru 3d doublet at 280.7 eV and 284.8 eV, and the C 1s peak at 286.5 eV due to the CO ligands. After annealing, CO desorbs and the ruthenium peaks shift to lower binding energies.

2H-TPP and $\text{Ru}_3(\text{CO})_{12}$ on Ag(111). To elucidate the origin of the self-terminating process we identified in our earlier work,¹⁰ we examined the metalation as a function of undecorated Ag(111) areas available to the precursor molecules. To this end surfaces with two different coverages each of pristine 2H-TPP (**3**) and planar 2H-TPP derivatives (**4**, **5**, **6**, **7**) were prepared, resulting in different free silver surface patches. The phenyl legs of pristine 2H-TPP (**3**) on Ag(111) are known to tilt with respect to the surface,²¹ which is corroborated by curve-fitting analysis of the angular dependence of π^* resonances in our angle-resolved NEXAFS measurements (Figure S3a), yielding an average tilt angle of $\sim 45^\circ$. Annealing to 550 K quenches the π^* resonances of the NEXAFS at 90° of photon incidence (Figure S3b),

1
2
3 due to the completion of intramolecular cyclodehydrogenation reactions which yield planar
4 2H-TPP derivatives (4, 5, 6, 7).^{10, 22} For ~ 1 ML of planar 2H-TPP derivatives, obtained by
5 dosing the molecules on a substrate kept at 550 K for prolonged time with high flux, the XPS
6 N 1s region shows two peaks at 397.9 eV (iminic) and 399.6 eV (aminic) (Figure 3a). It can
7 be noted that the aminic nitrogen peak has a slightly higher intensity than the iminic one. This
8 effect was already observed in the first XPS studies of porphyrins and attributed to the
9 presence of a weak satellite of the lower-energy peak which overlaps with that of the aminic
10 nitrogen.²³⁻²⁴ The (compared to pristine 2H-TPP, see below) reduced peak splitting of 1.7 eV
11 is consistent with our previous findings.¹⁰ After dosing Ru₃(CO)₁₂ only a very small amount
12 of Ru adsorbs (highlighted by the red peak in Figure 3b), whereas in the C 1s and N 1s
13 regions no difference can be detected. Consequently, following annealing to 550 K only a
14 small portion of the porphyrins gets metalated, as evidenced by the appearance of a weak
15 additional component (blue peak in Figure 3c left) at 398.7 eV, which is a typical binding
16 energy value for metalloporphyrins, while the signals originating from the nitrogen atoms of
17 the free-base species are slightly reduced. Conversely, for ~ 0.8 ML of planar 2H-TPP
18 derivatives (Figure 3d), the deposition of the precursor leads to a more pronounced
19 accumulation of Ru (red peak in Figure 3e, 280.6 eV and 281.1 eV) and (CO) (286.5 eV,
20 Figure 3e), indicating that Ru₃(CO)₁₂ adsorbs on the bare Ag(111) surface and does not bond
21 to the porphyrin areas at the employed conditions. Subsequent annealing to 550 K leads to a
22 fully metalated porphyrin layer on the surface, as evidenced by a single peak in the N 1s
23 spectrum (Figure 3g). Lower annealing temperatures only resulted in incomplete metalation
24 of the overlayer based on the N 1s spectrum (Figure 3f), which clearly exhibits residual
25 contributions of the iminic (orange peak) and aminic (green peak) N atoms, beside the major
26 component due to the metal coordinated nitrogen (blue peak). As in our earlier report,¹⁰ the
27 Ru peak shifts downward (to 279.6 eV) to a formal Ru⁰ state, after the metalation. This is in
28
29
30
31
32
33
34
35
36
37
38
39
40
41
42
43
44
45
46
47
48
49
50
51
52
53
54
55
56
57
58
59
60

1
2
3 agreement with the Ru oxidation state of pre-synthesized Ru-TPP adsorbed on Ag(111)
4 (Supporting information and Figure S4). It can also be noticed that the ratio of Ru 3d_{5/2} to C
5 1s of this surface closely matches the ratio of Ru 3d_{5/2} to C 1s of Ru-TPP (Supporting
6 information and Figure S4), indicating that all the surface Ru is engaged in porphyrin
7 macrocycles. Therefore the amount of surface Ru precursor **1** can be controlled by the
8 amount of free silver surface, and, specifically, approximately 20% of uncovered surface
9 silver ensures the complete metalation of the porphyrin layer without the accumulation of
10 excess Ru. This is in good agreement with a rough calculation based of the 2H-TPP
11 derivatives' (**4**, **5**, **6**, **7**) molecular surface footprints (~ 2 nm²) and the precursor (**1**) molecular
12 area (~ 1 nm²): Assuming that the precursor adsorbs only on the free silver surface and that
13 dense packing of the porphyrins and the precursor molecules can be achieved, complete
14 metalation requires ~14% of free silver surface (this represents, of course, a lower limit given
15 the approximation made). Accordingly the two cycles of exposure and annealing required for
16 the complete, self-limiting metalation protocol in our earlier work are rationalized: in fact, in
17 those porphyrin layers only ~12% of free silver surface was available.¹⁰ Excess Ru can
18 accumulate on the surface with a single exposure, if less than ~ 80% of the Ag surface is
19 covered.
20
21
22
23
24
25
26
27
28
29
30
31
32
33
34
35
36
37
38
39
40
41
42
43
44
45
46
47
48
49
50
51
52
53
54
55
56
57
58
59
60

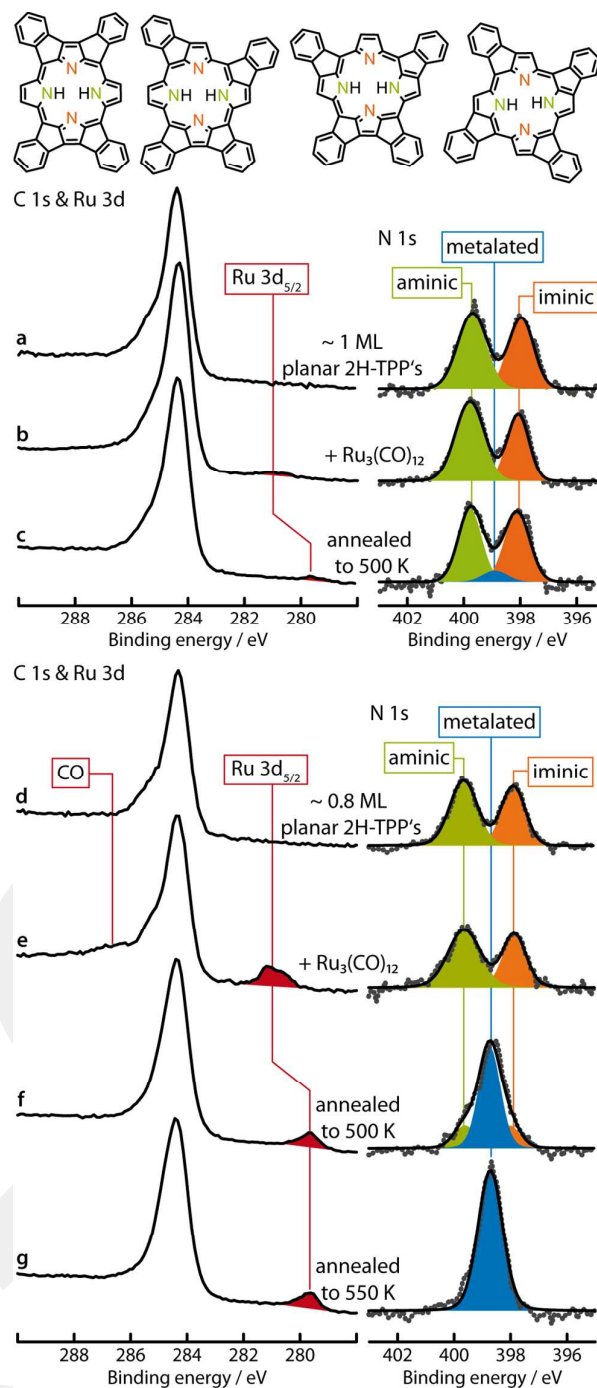


Figure 3: XPS spectra of the C 1s and Ru 3d (left) and N 1s (right) regions corresponding to: (a) ~ 1 ML of planar 2H-TPP derivatives on Ag(111) (b) after exposure to Ru₃(CO)₁₂ and after (c) annealing to 500 K and (d) ~ 0.8 ML of planar 2H-TPP derivatives on Ag(111) (e) after exposure to Ru₃(CO)₁₂ and (f) after annealing to 500 K and (g) 550 K.

1
2
3
4
5 Next, the coverage-dependent metalation of the pristine 2H-TPP on Ag(111) is presented.
6
7 To look into the adsorption behavior of the precursor on the 2H-TPP layer, a sample with a
8
9 2H-TPP coverage of ~ 1.3 ML was deposited on Ag(111). 2H-TPP adsorbed on Ag(111)
10
11 forms close-packed islands (Figure 5a),²⁵ so that it can be assumed that at this coverage no
12
13 bare silver is available. The XPS N 1s region shows two peaks at 398.1 eV (iminic) and
14
15 400.1 eV (aminic), i.e., a peak splitting of 2.0 eV (Figure S5a right), which is in full
16
17 agreement with literature data.²⁶⁻²⁸ After exposing this layer to the Ru₃(CO)₁₂ vapor no Ru
18
19 signal is detected, nor any change of the C 1s and N 1s spectra (Figure S5b), indicating that
20
21 the precursor molecules have a negligible sticking coefficient to the porphyrins at RT in
22
23 UHV. Consequently, after annealing to 530 K, no indication of metalation is found (Figure
24
25 S5c).
26
27
28

29
30 As it is now evident that the precursor does not adsorb (nor dissociates) on top of the 2H-
31
32 TPP at RT in UHV, we explored the metalation on a submonolayer coverage (~ 0.4 ML) of
33
34 2H-TPP on Ag(111) (Figure 4a). Dosing Ru₃(CO)₁₂ onto this surface hardly influences the N
35
36 1s region (Figure 4b right). In the C 1s region, however, additional peaks, which originate
37
38 from Ru 3d_{5/2} (280.5 eV and 281.0 eV) and CO (286.4 eV) (Figure 4b left), are clearly
39
40 discernible. The intensity of the C 1s porphyrin peak at 284.8 eV appears to be higher than
41
42 before, due to the overlap with the Ru 3d_{3/2} peaks. O 1s measurements (not displayed)
43
44 confirm the presence of oxygen on the sample. Annealing to 500 K causes the desorption of
45
46 CO (Figure 4c left) and a distinct downward shift of the Ru peaks. In the N 1s region, the
47
48 chemical state of Ru coordinated N appears at 398.8 eV (blue peak in Figure 4c right).
49
50
51
52
53
54
55
56
57
58
59
60

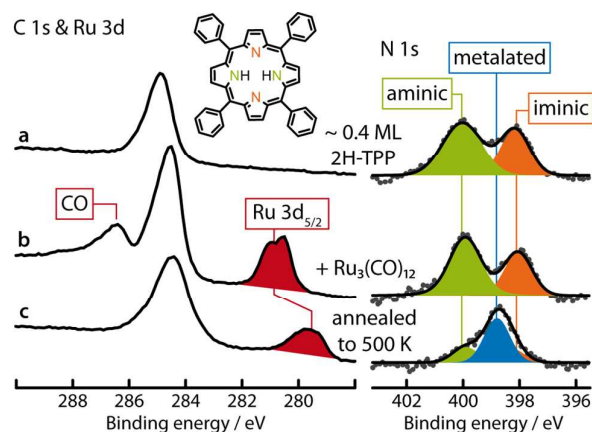


Figure 4. XP spectra of the metalation of 2H-TPP on Ag(111) with $\text{Ru}_3(\text{CO})_{12}$. (a) On the surface with a submonolayer coverage of 2H-TPP (b) a large amount of the precursor can accumulate (Ru $3d_{5/2}$ peak colored red). (c) After annealing to 500 K, the CO ligands desorb, the two N 1s peaks originating from the iminic (orange) and aminic (green) nitrogen species are quenched and a new peak (blue) emerges, which is assigned to the nitrogen in Ru porphyrins.

While at this temperature the metalation is not yet complete, the corresponding NEXAFS C K-edge spectra (Figure S3c) have changed substantially compared to the data of the untreated sample (Figure S3a). All curves appear broadened and the intensity of the 90° -curve in the π^* region is diminished, which indicates a more planar adsorption geometry. This broadening and angular dependence is not characteristic of the corresponding pristine Ru-TPP spectrum (Figure S3e), which reveals a saddle-shape conformation of the macrocycle and strongly rotated phenyl legs with respect to the surface plane. The origin of these changes might be the stronger interaction with the Ru modified silver substrate, but they might also originate from cyclodehydrogenation side reactions, which can have a lower activation barrier in the presence of surface ruthenium, as also observed in the presence of surface osmium.¹¹

1
2
3 To clarify this point, complementary STM measurements were performed. Figure 5a shows
4 a typical image of an island of 2H-TPP forming on the Ag(111) surface. Individual 2H-TPP
5 molecules can be resolved (examples outlined in blue in Figure 5a,b) with submolecular
6 resolution: the four protrusions in the periphery correspond to the tilted phenyl moieties,
7 whereas the central ring represents the macrocycle.²¹ The 2H-TPP molecules self-assemble in
8 close packed islands stabilized by T-type interactions between the phenyl legs.²⁹⁻³⁰ The STM
9 appearance of the surface depicted in Figure 5a after exposure to Ru₃(CO)₁₂ and annealing to
10 463 K is shown in Figure 5b. Here, intact 2H-TPP molecules can be identified (examples
11 circled in blue solid line) as well as the corresponding Ru-TPP molecule (one such molecule
12 circled in blue dashed line). However the outline of many molecules has changed (outlined in
13 green in Figure 5b), which signifies cyclodehydrogenation reactions between phenyl legs and
14 the macrocycle.³¹ The intramolecular cyclodehydrogenation reactions result in the phenyl
15 substituents being co-planar and therefore do not allow the T-type interactions that drive the
16 self-assembly observed in Figure 5a. This leads to an evident loss of order in the molecular
17 assembly. Importantly, it is further noted that this loss of order is not associated with the Ru
18 metalation, as Ru-TPP also forms the same structure as that observed in Figure 5a.³¹ A small
19 portion of the surface molecules exhibits a bright protrusion (e.g. circled in dashed lines in
20 Figure 5b) in the middle of the macrocycle ring, indicative of the insertion of Ru.¹⁰ After
21 further annealing of this surface to 493 K, we observe that the fraction of metalated
22 porphyrins has increased. At the same time, the majority of the porphyrins has completed all
23 the possible intramolecular cyclodehydrogenation reactions and the surface molecular species
24 are mainly the 2H-TPP derivatives **4**, **5**, **6**, **7** (Figure 1) and their Ru metalated counterparts.
25 These are identified by their match to the molecular structure outline and the apparent height
26 of their center (depression or protrusion). It is worth noting that the same
27 cyclodehydrogenation reaction requires an annealing treatment of ~ 550 K on the bare
28
29
30
31
32
33
34
35
36
37
38
39
40
41
42
43
44
45
46
47
48
49
50
51
52
53
54
55
56
57
58
59
60

Ag(111) surface,^{10, 31-32} but only ~ 423 K when the surface has been exposed to $\text{Os}_3(\text{CO})_{12}$.¹¹ We therefore conclude that the presence of surface Ru promotes these cyclodehydrogenation reactions, albeit less efficiently than the presence of surface Os.

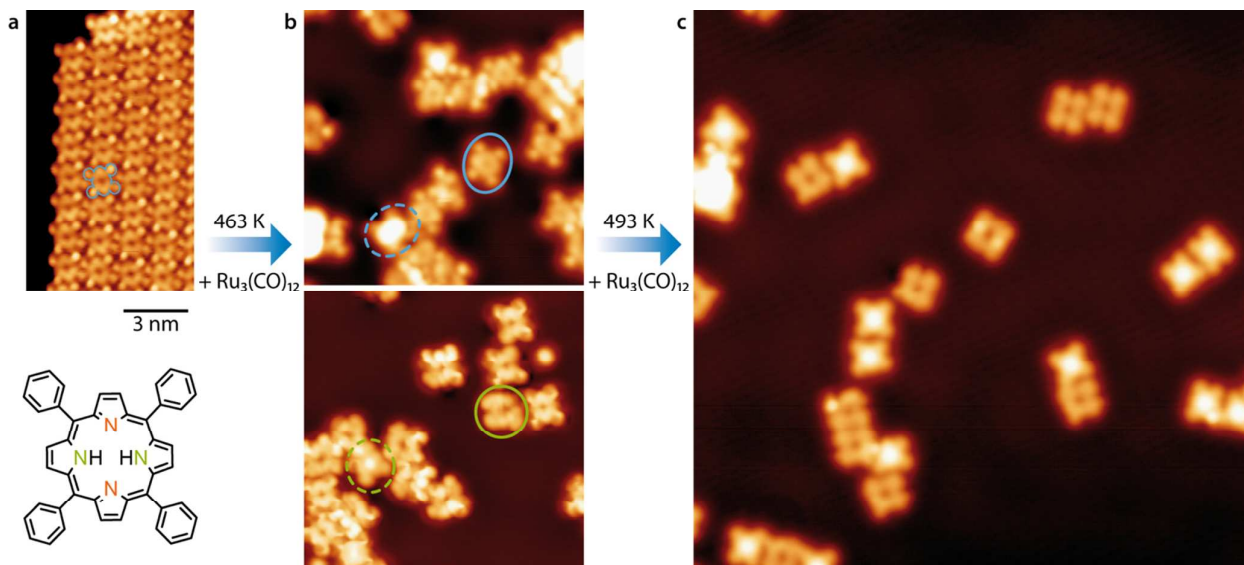


Figure 5. STM micrographs in the same scale of the reactants and products of the reaction of 2H-TPP (left) with $\text{Ru}_3(\text{CO})_{12}$ on Ag(111). (a) An island of 2H-TPP molecules ($T = 7$ K, $I = 0.14$ nA, $V_s = -0.43$ V). (b) The same surface after exposure to $\text{Ru}_3(\text{CO})_{12}$ and annealing to 463 K ($T = 7$ K, $I = 0.45$ nA, $V_s = -0.50$ V) and (c) after further annealing to 493 K ($T = 7$ K, $I = 0.13$ nA, $V_s = -0.50$ V).

2H-P on Ag(111). In a similar fashion we investigated the metalation of 2H-P. Similar to 2H-TPP and its derivatives, no metalation can be achieved without uncovered silver, because the $\text{Ru}_3(\text{CO})_{12}$ molecules do not adsorb on top of the porphine layer (not shown) under the employed conditions. For coverages below one monolayer, the N 1s data show that full metalation is possible (Figure 6e). Of special interest is hereby the C 1s region. For 2H-TPP the large number of inequivalent carbon atoms prevents a straightforward interpretation of the spectra. Instead, 2H-P contains only five inequivalent carbon species,³³ implying that changes upon annealing are more clearly discernible. Indeed, during the annealing series, the

1
2
3 C 1s core-level line undergoes a visible transformation. After deposition of the Ru precursor
4 and annealing to 470 K additional shoulders appear on both sides of the broad original peak
5 (Figure 6c). Notably, the fully metalated Ru-P layer exhibits two sharp peaks which are
6 reminiscent of the C 1s core-level spectra of 2H-P adsorbed on Cu(111)³³ and Cu-P/Cu(111)
7 (Figure S6). The second peak appears at lower binding energies, which is typical for a metal-
8 coordinated carbon species.³⁴ These results might suggest that after desorption of CO, mobile
9 Ru adatoms may diffuse below the porphine molecules, in such a way that we effectively
10 observe a Ru-P/Ru system. An alternative scenario is the coordination of Ru-P to ruthenium
11 to form chains, resulting in an organometallic surface network. Additionally, the presence of
12 the Ru on the surface appears to prevent a desorption of the molecules, as it was found that
13 the coverage of 2H-P on Ag(111) gradually decreases upon annealing (desorption rate at 533
14 K: $\sim 3\% \text{ ML}\cdot\text{min}^{-1}$)³⁵ which is not the case here.

15
16
17
18
19
20
21
22
23
24
25
26
27
28
29
30 The C K-edge NEXAFS spectra corresponding to the sample annealed to 505 K (Fig. S3d)
31 clearly correspond to that of a metalloporphine.³⁶⁻³⁷ In contrast to the C K-edge NEXAFS
32 spectrum of the Ru metalated planar TPP derivatives on Ag(111) discussed in the section
33 before and the 2H-P homocoupling reaction products on Ag(111),³⁵ the respective Ru-P
34 NEXAFS spectrum is only marginally broadened. This suggests that the broadening of the
35 NEXAFS spectra can be associated with extending the π conjugation of the molecule either
36 *via* cyclodehydrogenations or dimerization, rather than with the metalation process itself.
37
38
39
40
41
42
43
44
45
46
47
48
49
50
51
52
53
54
55
56
57
58
59
60
STM inspection of a similarly prepared surface (Figure 6f) revealed the formation of irregular
chains (two examples outlined by dotted green lines in Figure 6f), which were found to be
stable for imaging up to room temperature. In comparison, individual 2H-P molecules on
Ag(111) are too mobile to be imaged under similar tunneling conditions even at ~ 113 K.
Only a few free base species, characterized by an asymmetric ring with a characteristic
depression,³⁸ can be identified within these chains (circled in blue), suggesting that the

majority of molecules is metalated. The STM image does not allow to unambiguously identify the monomers within the chains, therefore the intermolecular distances cannot be deduced. However, based on the corresponding NEXAFS spectroscopic signature and the changes in the C 1s XPS region discussed above we can propose that these chains are stabilized by interactions between Ru atoms and porphine molecules, rather than by intermolecular C-C couplings observed in our earlier work.³⁵

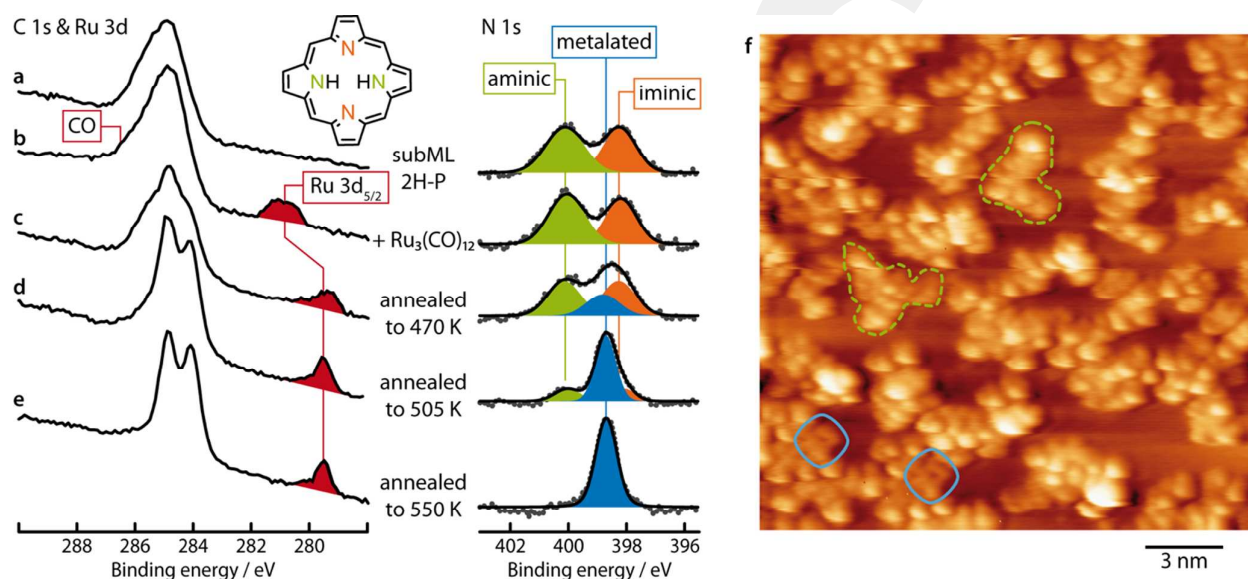


Figure 6. Metalation of 2H-P/Ag(111) with Ru₃(CO)₁₂. (a-e) Sequential spectra for the C 1s and N 1s core levels. The Ru 3d_{5/2} peak is colored red. Annealing leads to the formation of Ru-P, as indicated by the growth of a new peak (blue, 398.8 eV) in the N 1s spectra. (f) STM ($T = 95$ K, $I = 0.05$ nA, $V_s = -1.07$ V) image of Ru-P on Ag(111) after dosing Ru₃(CO)₁₂ and annealing to 500 K.

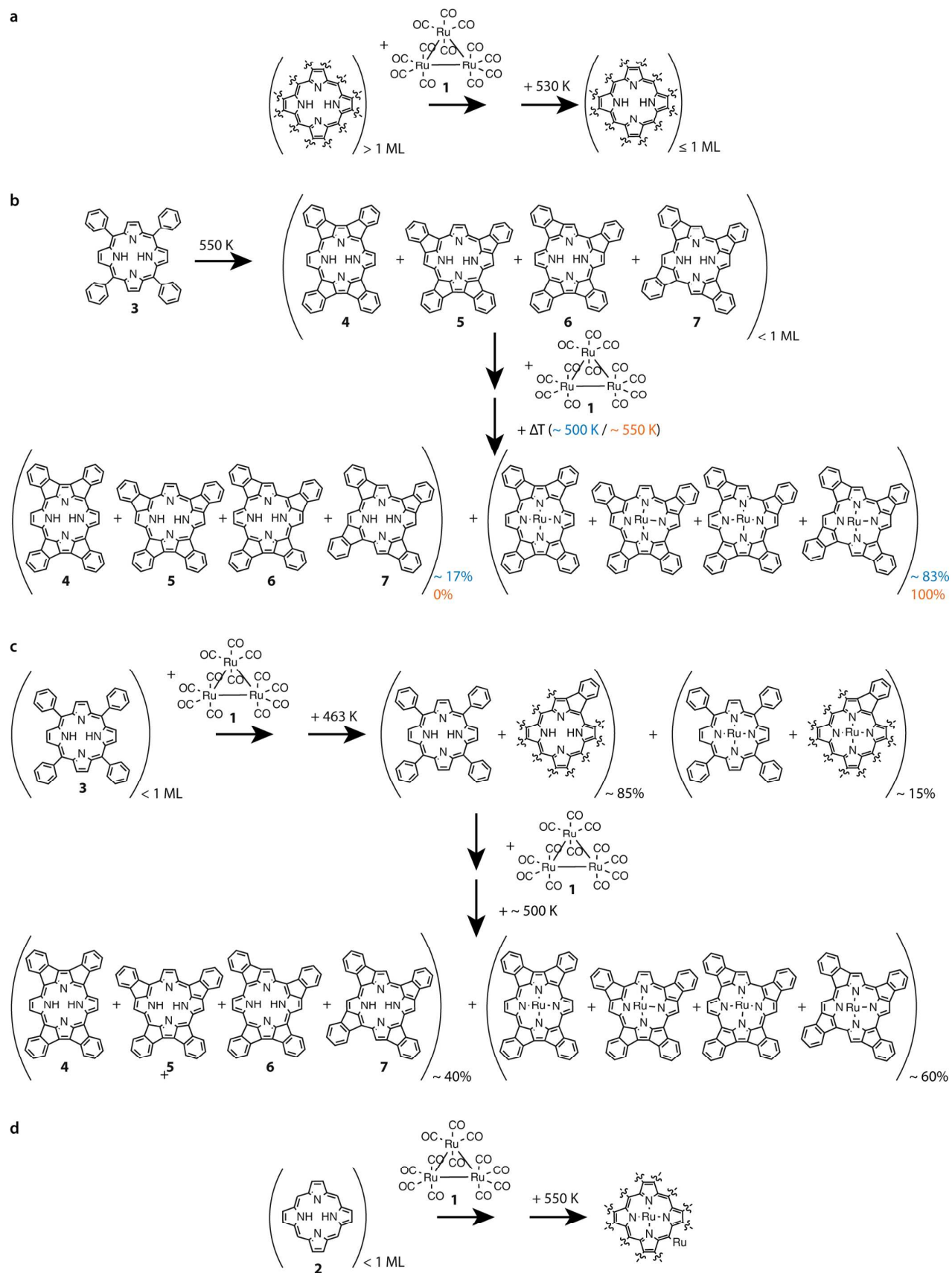
4. CONCLUSIONS

Our key findings are summarized in Figure 7. We have shown that metalation by metal-organic CVD is possible for 2H-TPP, its high-temperature planar cyclodehydrogenated 2H-TPP derivatives and 2H-P. For all three compounds annealing temperatures of 550 K were required for a complete metalation. Coverage dependent measurements reveal that the crucial

1
2
3 point is the amount of bare silver available, as the $\text{Ru}_3(\text{CO})_{12}$ precursor neither adsorbs nor
4
5 transforms on top of the molecules under UHV at RT. For all coverages of free-base
6
7 porphyrins, as well as for the pure $\text{Ru}_3(\text{CO})_{12}$ compound, no carbon monoxide could be
8
9 detected after annealing to 550 K. Excess Ru can accumulate on the surface depending on the
10
11 surface concentration of adsorbed Ru precursor. The latter can be controlled either by the
12
13 dosing time or by the free silver surface. Moreover, the critical role of the silver surface in the
14
15 CVD metalation process was elucidated. The porphyrin metalation temperatures coincide
16
17 with the formation of adsorbed metallic Ru. Therefore a reaction mechanism can be
18
19 confidently proposed: the Ru precursor adsorbs on the bare Ag surface, where it thermally
20
21 decomposes resulting in reactive Ru atoms which metalate surface porphyrin species. As the
22
23 sticking of $\text{Ru}_3(\text{CO})_{12}$ is limited to the free silver at RT under UHV, higher porphyrin
24
25 coverages mean that the accumulation of Ru under these conditions and consequently the
26
27 reaction can become self-limiting. This constitutes a big advantage over the use of electron
28
29 beam evaporators for the deposition of the metal atoms, for which the dosage of the exact
30
31 metal amount is an additional challenge. The XPS and NEXAFS data of pre-synthesized Ru-
32
33 TPP point to a saddle-shaped molecular conformation on Ag(111), as well as to a reduction
34
35 of the formal +2 state of the ruthenium in the free porphyrin to Ru^0 in the molecules directly
36
37 in contact with the silver substrate, which presumably reflects charge transfer between
38
39 substrate and molecules. The same result is found for *in vacuo* metalated porphyrins,
40
41 indicating that the apparent oxidation state is not drastically influenced by the height of the
42
43 molecules above the substrate, which can be expected to be different for the pristine TPP
44
45 species with tilted phenyl substituents on the one hand, and the planar 2H-TPP derivatives
46
47 and 2H-P on the other hand. Finally, we observed that surface Ru additionally interacts with
48
49 the peripheral carbon atoms of the porphyrin molecules. For the 2H-TPP, it lowers the
50
51
52
53
54
55
56
57
58
59
60

1
2
3 activation barrier of the intramolecular cyclodehydrogenation reactions, whereas for the 2H-
4
5 P, it likely induces the formation of metal-organic chains.
6
7
8
9
10
11
12
13
14
15
16
17
18
19
20
21
22
23
24
25
26
27
28
29
30
31
32
33
34
35
36
37
38
39
40
41
42
43
44
45
46
47
48
49
50
51
52
53
54
55
56
57
58
59
60

GCPRIS



1
2
3 **Figure 7.** Summary of surface reactions observed here between porphyrin molecules
4 supported on Ag(111) and the metal precursor **1** under UHV conditions. (a) For porphyrin
5 coverages above a monolayer no reaction is observed. (b) The 2H-TPP derivatives **4, 5, 6, 7**
6 metalate after heating to 500 K and is completed after heating to 550 K. (c) In 2H-TPP both
7 metalation and cyclodehydrogenations occur after heating to 463 K. All possible 2H-TPP
8 cyclodehydrogenations are completed after heating to 500 K. (d) 2H-P both metalates and
9 coordinates to Ru atoms.
10
11
12
13
14
15
16
17

18 ASSOCIATED CONTENT

19
20
21
22 **Supporting Information.** Raw data of N 1s spectra; experimental: NEXAFS; NEXAFS C
23 K-edge spectra; XPS and NEXAFS of Ru-TPP on Ag(111); XP spectra of Ru-TPP on
24 Ag(111); absence of Ru₃(CO)₁₂ on multilayer 2H-TPP on Ag(111); XP spectra; C 1s of 2H-P
25 and Cu-P on Cu(111). This material is available free of charge via the Internet at
26 <http://pubs.acs.org>.
27
28
29
30
31
32

33 Notes

34
35
36 The authors declare no competing financial interests.
37
38

39 ACKNOWLEDGMENT

40
41
42
43 We thank Helmholtz-Zentrum Berlin (HZB) for the allocation of synchrotron radiation
44 beamtime and financial support. The authors thank Peter Feulner for assistance during the
45 synchrotron experiments, and Alexei Nefedov and Christof Wöll for access to the HE-SGM
46 end station. This work was supported by the EU FP7 program through the European Research
47 Council Advanced Grant MolArt (J.V.B, no. 247299) and the Marie Curie Fellowships
48 NASUMECA (A.C.P., no. 274842) and NANOULOP (Ö.S., no. 302157). Further funding
49 was provided by the Munich-Centre for Advanced Photonics (project B.1.3), the TUM-IAS
50
51
52
53
54
55
56
57
58
59
60

(W.A.) and the International Max Planck Research School of Advanced Photon Science (IMPRS-APS) (A.W.).

REFERENCES

1. Auwärter, W.; Écija, D.; Klappenberger, F.; Barth, J. V., Porphyrins at Interfaces. *Nat. Chem.* **2015**, *7*, 105-120.
2. Gottfried, J. M., Surface Chemistry of Porphyrins and Phthalocyanines. *Surf. Sci. Rep.* **2015**, *70*, 259-379.
3. Marbach, H., Surface-Mediated *in Situ* Metalation of Porphyrins at the Solid–Vacuum Interface. *Acc. Chem. Res.* **2015**, *48*, 2649-2658.
4. Diller, K.; Papageorgiou, A. C.; Klappenberger, F.; Allegretti, F.; Barth, J. V.; Auwärter, W., In Vacuo Interfacial Tetrapyrrole Metallation. *Chem. Soc. Rev.* **2016**, *45*, 1629-1656.
5. Weber-Bargioni, A.; Reichert, J.; Seitsonen, A. P.; Auwärter, W.; Schiffrin, A.; Barth, J. V., Interaction of Cerium Atoms with Surface-Anchored Porphyrin Molecules. *J. Phys. Chem. C* **2008**, *112*, 3453-3455.
6. Auwärter, W.; Weber-Bargioni, A.; Brink, S.; Riemann, A.; Schiffrin, A.; Ruben, M.; Barth, J. V., Controlled Metalation of Self-Assembled Porphyrin Nanoarrays in Two Dimensions. *ChemPhysChem* **2007**, *8*, 250-254.
7. Gottfried, J. M.; Flechtner, K.; Kretschmann, A.; Lukasczyk, T.; Steinrück, H.-P., Direct Synthesis of a Metalloporphyrin Complex on a Surface. *J. Am. Chem. Soc.* **2006**, *128*, 5644-5645.

1
2
3 8. Diller, K.; Klappenberger, F.; Marschall, M.; Hermann, K.; Nefedov, A.; Wöll, C.;
4
5 Barth, J. V., Self-Metalation of 2H-tetraphenylporphyrin on Cu(111): An X-Ray
6
7 Spectroscopy Study. *J. Chem. Phys.* **2012**, *136*, 014705-13.
8

9
10 9. Goldoni, A.; Pignedoli, C. A.; Di Santo, G.; Castellarin-Cudia, C.; Magnano, E.;
11
12 Bondino, F.; Verdini, A.; Passerone, D., Room Temperature Metalation of 2H-TPP
13
14 Monolayer on Iron and Nickel Surfaces by Picking up Substrate Metal Atoms. *ACS Nano*
15
16 **2012**, *6*, 10800-10807.
17

18
19
20 10. Papageorgiou, A. C.; Fischer, S.; Oh, S. C.; Sağlam, Ö.; Reichert, J.; Wiengarten, A.;
21
22 Seufert, K.; Vijayaraghavan, S.; Écija, D.; Auwärter, W., et al., Self-Terminating Protocol for
23
24 an Interfacial Complexation Reaction *in Vacuo* by Metal–Organic Chemical Vapor
25
26 Deposition. *ACS Nano* **2013**, *7*, 4520-4526.
27

28
29
30 11. Sağlam, Ö.; Yetik, G.; Reichert, J.; Barth, J. V.; Papageorgiou, A. C., On-Surface
31
32 Reaction of Tetraphenylporphyrins with Os₃(CO)₁₂ Precursors and Os Clusters: A Scanning
33
34 Tunnelling Microscopy Investigation. *Surf. Sci.* **2016**, *646*, 26-30.
35

36
37 12. Kulkarni, A.; Lobo-Lapidus, R. J.; Gates, B. C., Metal Clusters on Supports:
38
39 Synthesis, Structure, Reactivity, and Catalytic Properties. *Chem. Commun.* **2010**, *46*, 5997-
40
41 6015.
42

43
44 13. Pollak, R. A.; Ley, L.; McFeely, F. R.; Kowalczyk, S. P.; Shirley, D. A.,
45
46 Characteristic Energy Loss Structure of Solids from X-Ray Photoemission Spectra. *J.*
47
48 *Electron Spectrosc. Relat. Phenom.* **1974**, *3*, 381-398.
49

50
51
52 14. Anderson, A. E.; Grillo, F.; Larrea, C. R.; Seljamäe-Green, R. T.; Früchtl, H. A.;
53
54 Baddeley, C. J., Metallosupramolecular Assembly of Cr and *p*-Terphenyldinitrile by
55
56 Dissociation of Metal Carbonyls on Au(111). *J. Phys. Chem. C* **2016**, *120*, 1049-1055.
57
58
59
60

1
2
3 15. Diller, K. Free-Base and Metalated Porphyrins on Metal Surfaces - a Systematic X-
4 Ray Spectroscopy and Density Functional Theory Investigation. Technische Universität
5 München, München, 2013.
6
7

8
9
10 16. Mårtensson, N.; Nyholm, R.; Johansson, B., New Observation of Two-Hole Core-
11 Level Satellites in Copper, Silver, and Gold. *Phys. Rev. B* **1984**, *29*, 4800-4802.
12
13

14
15 17. Stadler, C.; Hansen, S.; Pollinger, F.; Kumpf, C.; Umbach, E.; Lee, T. L.;
16 Zegenhagen, J., Structural Investigation of the Adsorption of SnPc on Ag(111) Using
17 Normal-Incidence X-Ray Standing Waves. *Phys. Rev. B* **2006**, *74*, 035404.
18
19

20
21 18. Vaari, J.; Lahtinen, J.; Hautojärvi, P., A Bimetallic Ru–Co Surface Prepared by
22 Ru₃(CO)₁₂ Adsorption on Co(0001). *Surf. Sci.* **1996**, *346*, 11-17.
23
24

25
26 19. Cai, T.; Song, Z.; Chang, Z.; Liu, G.; Rodriguez, J. A.; Hrbek, J., Ru Nanoclusters
27 Prepared by Ru₃(CO)₁₂ Deposition on Au(1 1 1). *Surf. Sci.* **2003**, *538*, 76-88.
28
29

30
31 20. Wagner, C. D.; Riggs, W. M.; Davis, L. E.; Moulder, J. F.; Muilenberg, G. E.,
32 *Handbook of X-Ray Photoelectron Spectroscopy : A Reference Book of Standard Data for*
33 *Use in X-Ray Photoelectron Spectroscopy*; Perkin-Elmer Corporation: U.S.A., 1979.
34
35

36
37 21. Auwärter, W.; Seufert, K.; Bischoff, F.; Écija, D.; Vijayaraghavan, S.; Joshi, S.;
38 Klappenberger, F.; Samudrala, N.; Barth, J. V., A Surface-Anchored Molecular Four-Level
39 Conductance Switch Based on Single Proton Transfer. *Nat. Nanotechnol.* **2012**, *7*, 41-46.
40
41

42
43 22. Di Santo, G.; Sfiligoj, C.; Castellarin-Cudia, C.; Verdini, A.; Cossaro, A.; Morgante,
44 A.; Floreano, L.; Goldoni, A., Changes of the Molecule–Substrate Interaction Upon Metal
45 Inclusion into a Porphyrin. *Chem. – Eur. J.* **2012**, *18*, 12619-12623.
46
47
48
49
50
51
52
53
54
55
56
57
58
59
60

1
2
3 23. Karweik, D. H.; Winograd, N., Nitrogen Charge Distributions in Free-Base
4 Porphyrins, Metalloporphyrins, and Their Reduced Analogs Observed by X-Ray
5 Photoelectron Spectroscopy. *Inorg. Chem.* **1976**, *15*, 2336-2342.
6
7

8
9
10 24. Niwa, Y.; Kobayashi, H.; Tsuchiya, T., X-Ray Photoelectron Spectroscopy of
11 Tetraphenylporphin and Phthalocyanine. *J. Chem. Phys.* **1974**, *60*, 799-807.
12
13

14
15 25. Rojas, G.; Simpson, S.; Chen, X.; Kunkel, D. A.; Nitz, J.; Xiao, J.; Dowben, P. A.;
16 Zurek, E.; Enders, A., Surface State Engineering of Molecule-Molecule Interactions. *Phys.*
17 *Chem. Chem. Phys.* **2012**, *14*, 4971-4976.
18
19

20
21 26. Buchner, F.; Flechtner, K.; Bai, Y.; Zillner, E.; Kellner, I.; Steinrück, H.-P.; Marbach,
22 H.; Gottfried, J. M., Coordination of Iron Atoms by Tetraphenylporphyrin Monolayers and
23 Multilayers on Ag(111) and Formation of Iron-Tetraphenylporphyrin. *J. Phys. Chem. C*
24 **2008**, *112*, 15458-15465.
25
26

27
28 27. Gottfried, J. M.; Flechtner, K.; Kretschmann, A.; Lukasczyk, T.; Steinrück, H.-P.,
29 Direct Synthesis of a Metalloporphyrin Complex on a Surface. *J. Am. Chem. Soc.* **2006**, *128*,
30 5644-5645.
31
32

33
34 28. Shubina, T. E.; Marbach, H.; Flechtner, K.; Kretschmann, A.; Jux, N.; Buchner, F.;
35 Steinrück, H.-P.; Clark, T.; Gottfried, J. M., Principle and Mechanism of Direct Porphyrin
36 Metalation: Joint Experimental and Theoretical Investigation. *J. Am. Chem. Soc.* **2007**, *129*,
37 9476-9483.
38
39

40
41 29. Auwärter, W.; Seufert, K.; Klappenberger, F.; Reichert, J.; Weber-Bargioni, A.;
42 Verdini, A.; Cvetko, D.; Dell'Angela, M.; Floreano, L.; Cossaro, A., et al., Site-Specific
43 Electronic and Geometric Interface Structure of Co-tetraphenyl-porphyrin Layers on
44 Ag(111). *Phys. Rev. B* **2010**, *81*, 245403.
45
46
47
48
49

1
2
3 30. Buchner, F.; Kellner, I.; Hieringer, W.; Görling, A.; Steinrück, H.-P.; Marbach, H.,
4
5 Ordering Aspects and Intramolecular Conformation of Tetraphenylporphyrins on Ag(111).
6
7 *Phys. Chem. Chem. Phys.* **2010**, *12*, 13082-13090.

8
9
10 31. Wiengarten, A.; Lloyd, J. A.; Seufert, K.; Reichert, J.; Auwärter, W.; Han, R.;
11
12 Duncan, D. A.; Allegretti, F.; Fischer, S.; Oh, S. C., et al., Surface-Assisted
13
14 Cyclodehydrogenation; Break the Symmetry, Enhance the Selectivity. *Chem. – Eur. J.* **2015**,
15
16 *21*, 12285-12290.

17
18
19 32. Di Santo, G.; Blankenburg, S.; Castellarin-Cudia, C.; Fanetti, M.; Borghetti, P.;
20
21 Sangaletti, L.; Floreano, L.; Verdini, A.; Magnano, E.; Bondino, F., et al., Supramolecular
22
23 Engineering through Temperature-Induced Chemical Modification of 2H-
24
25 Tetraphenylporphyrin on Ag(111): Flat Phenyl Conformation and Possible Dehydrogenation
26
27 Reactions. *Chem. – Eur. J.* **2011**, *17*, 14354-14359.

28
29
30 33. Diller, K.; Klappenberger, F.; Allegretti, F.; Papageorgiou, A. C.; Fischer, S.; Duncan,
31
32 D. A.; Maurer, R. J.; Lloyd, J. A.; Oh, S. C.; Reuter, K., et al., Temperature-Dependent
33
34 Templated Growth of Porphine Thin Films on the (111) Facets of Copper and Silver. *J.*
35
36 *Chem. Phys.* **2014**, *141*, 144703.

37
38
39 34. Zhang, Y.-Q.; Kepčija, N.; Kleinschrodt, M.; Diller, K.; Fischer, S.; Papageorgiou, A.
40
41 C.; Allegretti, F.; Björk, J.; Klyatskaya, S.; Klappenberger, F., et al., Homo-Coupling of
42
43 Terminal Alkynes on a Noble Metal Surface. *Nat. Commun.* **2012**, *3*, 1286.

44
45
46 35. Wiengarten, A.; Seufert, K.; Auwärter, W.; Eciija, D.; Diller, K.; Allegretti, F.;
47
48 Bischoff, F.; Fischer, S.; Duncan, D. A.; Papageorgiou, A. C., et al., Surface-Assisted
49
50 Dehydrogenative Homocoupling of Porphine Molecules. *J. Am. Chem. Soc.* **2014**, *136*, 9346-
51
52 9354.
53
54
55
56
57
58
59
60

1
2
3 36. Diller, K.; Klappenberger, F.; Allegretti, F.; Papageorgiou, A. C.; Fischer, S.;
4
5 Wiengarten, A.; Joshi, S.; Seufert, K.; Écija, D.; Auwärter, W., et al., Investigating the
6
7 Molecule-Substrate Interaction of Prototypic Tetrapyrrole Compounds: Adsorption and Self-
8
9 Metalation of Porphine on Cu(111). *J. Chem. Phys.* **2013**, *138*, 154710.

10
11
12 37. Krasnikov, S. A.; Sergeeva, N. N.; Brzhezinskaya, M. M.; Preobrajenski, A. B.;
13
14 Sergeeva, Y. N.; Vinogradov, N. A.; Cafolla, A. A.; Senge, M. O.; Vinogradov, A. S., An X-
15
16 Ray Absorption and Photoemission Study of the Electronic Structure of Ni Porphyrins and Ni
17
18 N-Confused Porphyrin. *J. Phys.: Condens. Matter* **2008**, *20*, 235207.

19
20
21 38. Bischoff, F.; Seufert, K.; Auwärter, W.; Joshi, S.; Vijayaraghavan, S.; Écija, D.;
22
23 Diller, K.; Papageorgiou, A. C.; Fischer, S.; Allegretti, F., et al., How Surface Bonding and
24
25 Repulsive Interactions Cause Phase Transformations: Ordering of a Prototype Macrocyclic
26
27 Compound on Ag(111). *ACS Nano* **2013**, *7*, 3139-3149.

